Plant Growth Regul (2018) 84:169–178
DOI 10.1007/s10725-017-0330-z

ORIGINAL PAPER

The calmodulin gene *AmCaM* from *Ammopiptanthus mongolicus* confers freezing and heat tolerance in *Escherichia coli*

Tingqiao Yu[1] · Guanhua Zhi[1] · Junna Shi[1] · Yuzhen Chen[1] · Man Shen[2] · Cunfu Lu[1]

Received: 26 November 2016 / Accepted: 24 September 2017 / Published online: 27 October 2017
© Springer Science+Business Media B.V. 2017

Abstract *Ammopiptanthus mongolicus* is an evergreen xerophytic shrub in the legume family, Fabaceae, growing in Mid-Asian desert regions. Previously, we reported the isolation and characterization of ESTs from *A. mongolicus* for a large number of cold and drought-responsive gene sequences. Based on this, we selected a calmodulin (CaM) gene (designated *AmCaM*) for functional characterization. Bioinformatic analysis revealed that the full-length ORF of *AmCaM* was 450 bp and encoded 149 amino acids. Phylogenetic analysis revealed that the AmCaM protein showed high identity to homologs from *Oryza sativa* and *Zea mays*, and to the homolog from the leguminous species *Vigna angularis*. Quantitative RT-PCR analysis showed that *AmCaM* transcription was enhanced under both cold and heat stress conditions. The *AmCaM* gene was transformed into *Escherichia coli* cells for functional characterization. Heterologous expression of *AmCaM* improved freezing and heat tolerance of the transformant *E. coli* cells. These results indicate that *AmCaM* contributes to enhanced freezing and heat tolerance and suggest that it is a candidate gene for engineering of abiotic stress tolerance in crop, woody, or ornamental plants.

Keywords *Ammopiptanthus mongolicus* · *AmCaM* gene · *Escherichia coli* · Heat and cold stress

Introduction

Calcium ions (Ca^{2+}) participate in intracellular signal transduction pathways that regulate diverse cellular processes. A variety of extracellular stimuli promote Ca^{2+}-mediated signal transduction, which activates exocytosis, contraction, metabolism, transcription, and fertilization and cell proliferation. Calcium signaling operates over a wide temporal range from microseconds to minutes or hours. The main toolkit components of Ca^{2+}-signaling systems in mammalian cells include receptors, transducers, channels, calcium buffers, calcium effectors, calcium-sensitive enzymes and processes, calcium pumps and exchangers (Berridge et al. 2003). However, the components of Ca^{2+}-signaling systems in plants remain incompletely known.

Three major EF-hand Ca^{2+} sensors have been characterized in plants, namely calmodulin (CaM) (Reddy et al. 2011), calcium-dependent protein kinase (CDPK) (Harmon et al. 2002) and calcineurin B-like protein (CBL) (Luan et al. 2002). The highly conserved CaM protein family, which is critical for many organisms, comprises multifunctional cytoplasmic Ca^{2+}-sensors that affect signaling cascades and responses to environmental stimuli by regulating target proteins or intracellular Ca^{2+} concentrations in eukaryotes (Benoit et al. 2006). Many studies have suggested that Ca^{2+} signaling influences plant response to abiotic stresses (Ali et al. 2017), including osmotic stress (Das et al. 2016; Kang et al. 2017), mechanical stimuli, salinity (Tian et al. 2015), and cold and heat shock (Dubrovina et al. 2017), and is involved in the regulation of multiple modes of cell death (Fasano et al. 2002; Gilroy et al. 2016). Transgenic

Electronic supplementary material The online version of this article (doi:10.1007/s10725-017-0330-z) contains supplementary material, which is available to authorized users.

✉ Cunfu Lu
lucunfu@bjfu.edu.cn

[1] Beijing Advanced Innovation Center for Tree Breeding by Molecular Design, College of Biological Sciences and Biotechnology, National Engineering Laboratory for Tree Breeding, Beijing Forestry University, Beijing 100083, China

[2] College of Plant Science and Technology, Beijing University of Agriculture, Beijing 102206, China

Arabidopsis thaliana plants overexpressing *AtCaMBP25* reportedly exhibit inhibited seed germination and root elongation when grown on stress-inducing media, indicating *AtCaMBP25* negatively affects osmotic and salt-stress responses (Perruc et al. 2004). In contrast to animals, plants possess a suite of CaM and CaM-like genes that encode CaM isoforms (Snedden and Fromm 2001). The *A. thaliana* genome includes the following seven genes that encode four types of CaM isoforms, which differ by 1–5 amino acid residues: *CaM1/4, CaM2/3/5, CaM6*, and *CaM7* (Bender and Snedden 2013; Abbas et al. 2014; Zhu et al. 2015). Additionally, five *CaM* genes have been identified in the rice genome (Boonburapong and Buaboocha 2007; Chinpongpanich et al. 2012). However, most of the identified plant *CaM* genes are from herbaceous species, and only a few *CaM* genes have been cloned from woody plants (Sun et al. 2011; Xu et al. 2014).

Experimental studies in our laboratory have focused on an extreme xerophyte, *A. mongolicus*, in an effort to identify and characterize novel genes involved in abiotic stress tolerance (Liu et al. 2013; Shi et al. 2016). *A. mongolicus* is an endangered shrub belonging to the Fabaceae believed to have originated in the Tertiary period (from 65 to 2 million years ago). The species inhabits primarily desert in northwestern China where the annual precipitation is often < 50–100 mm, and the temperature ranges from −30 °C in winter to 40 °C in summer (Wang et al. 2008; Liu et al. 2013). Given the ancient origin of the species and its survival in a persistently arid environment, this species is valuable for elucidation of mechanisms involved in drought adaptation and resistance. Therefore, *A. mongolicus* is a potentially useful resource for the study of abiotic stress-responsive genes.

We previously identified 5282 expressed sequence tags (ESTs) and 1594 unigenes responsive to cold conditions in the *Ammopiptanthus mongolicus* genome (Liu et al. 2013). We also characterized many genes associated with abiotic stress tolerance (Liu et al. 2010; Shi et al. 2016). The *A. mongolicus* EST database contains numerous genes that may be important for adaptations to abiotic stress conditions in desert-like environments. Thus, the *A. mongolicus* genome may be useful as a genetic resource for enhancing the abiotic stress tolerance of crop plants. In this study, we isolated and characterized an *A. mongolicus CaM* gene. Furthermore, this gene was heterologously expressed in *Escherichia coli* cells to examine its response to cold or heat stress.

Materials and methods

Bioinformatic analysis

The complete *A. mongolicus CaM* coding sequence (designated *AmCaM*) was derived from previously described ESTs (Liu et al. 2013) (Fig. 1). Sequence homologies were analyzed using BLAST searches of the National Center for Biotechnology Information databases (https://blast.ncbi.nlm.nih.gov/Blast.cgi). Fifty homologous proteins were downloaded from https://www.ncbi.nlm.nih.gov/. A multiple sequence alignment was generated with Clustal W as implemented in BioEdit 6.0. A phylogram was inferred using the maximum likelihood (ML) statistical method on the basis of the JTT matrix-based model using MEGA 5.0 (Tamura et al. 2011). A conserved domain analysis was conducted using the online Conserved Domain Database (http://www.ncbi.nlm.nih.gov/cdd/). The secondary and tertiary structure, and physical and chemical properties of the inferred protein were predicted with Expasy (http://www.expasy.org/).

Plant materials and treatments

Ammopiptanthus mongolicus seeds collected from the Alashan Desert, Inner Mongolian Autonomous Region of China, were germinated in a greenhouse (25 ± 5 °C, 16 h photoperiod and 30 ± 10% relative humidity). Twenty-day-old seedlings were subjected to different cold and heat stress treatments (4 °C for 0, 1, 2, 4, 8, 12 or 16 h, and 40 °C for 0, 1, 2, 4, 8, or 12 h). The leaves were harvested at the specified time points and stored at −80 °C.

RNA extraction and qRT-PCR analysis

Total RNA was isolated from frozen tissue using the EZgene™ Plant Easy Spin RNA Miniprep Kit following the manufacturer's instructions (Biomiga, San Diego, CA, USA). The absorbance at 260 nm was measured using a NanoDrop 2000 spectrophotometer to ensure equal concentrations of RNA from each tissue sample. Total RNA was used to synthesize cDNA with the oligo-(dT) primer using the TranScript® One-Step gDNA Removal and cDNA Synthesis SuperMix (TransGen Biotech, Beijing, China) following the manufacturer's instructions. Quantitative real-time PCR (qRT-PCR) analysis of the cDNA was performed on a CFX96 Real-Time System (Bio-RAD, Hercules, CA, USA) with *AmCaM* gene-specific primers (Table S1) and the TaKaRa SYBR® Premix Ex Taq™ (Takara) in accordance with the manufacturer's instructions. The *Actin* gene was selected for normalization using gene-specific primers listed in Table S1. All experiments were run in triplicate. Data were analyzed using the comparative Ct method and are presented as relative fold gene expression ($2^{-\Delta\Delta Ct}$) with three replicates.

Construction of pTWIN1-CaM plasmid

The *A. mongolicus CaM* gene sequence (GenBank accession number KX379686) was obtained from the

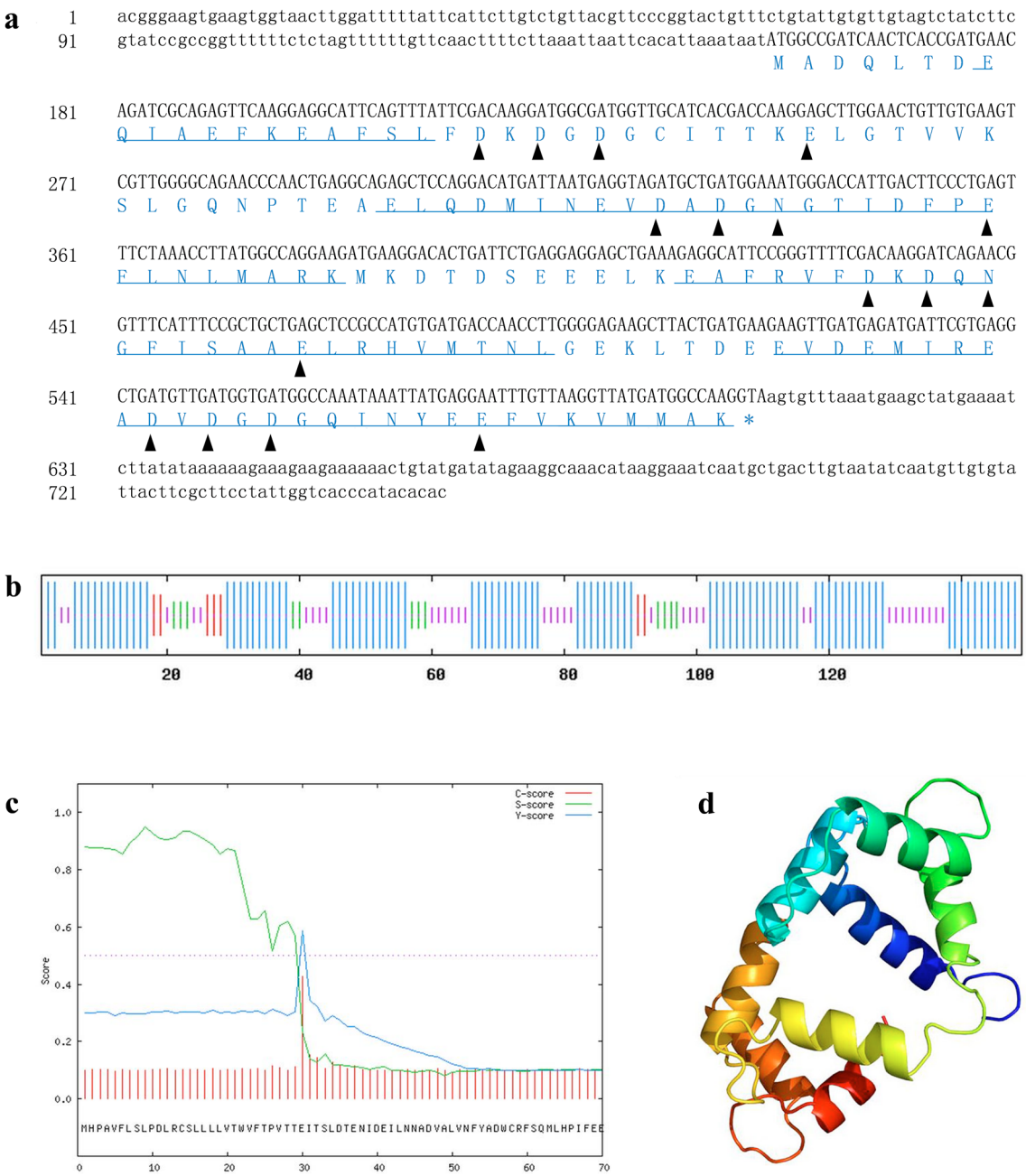

Fig. 1 Details regarding the *AmCaM* cDNA and deduced amino acid sequences. **a** *AmCaM* cDNA sequence derived from ESTs. The sequence in uppercase letters represents the complete ORF, while the sequences in lowercase letters before and after the ORF correspond to the 5′- and 3′-UTRs, respectively. The sequences in black and blue uppercase letters represent the coding and protein sequences, respectively. The four predicted EF-hand motifs are underlined and the conserved residues involved in Ca^{2+}-binding are indicated with closed triangles. **b** Sopma secondary structure prediction. The α-helices and extended strands are indicated by blue and red bars, respectively, whereas the green bars represent the random coil running through the whole molecule. **c** Signal peptide prediction (SignalP 4.1). A signal peptide cleavage site was detected between positions 29 and 30. **d** Predicted tertiary structure (Phyre 2). Image colored by rainbow N→C terminus; model dimensions (Å): X: 41.248, Y: 49.096, Z: 38.08. (Color figure online)

cold- and drought-induced EST database. A pair of primers (*AmCaM*-F* and *AmCaM*-R*) was designed based on the *AmCaM* cDNA sequence to amplify the full-length *AmCaM* sequence and insert it into the pTWIN1 vector (Table S1). The PCR amplification was completed using the following program: 25 cycles of 94 °C for 30 s, 54 °C for 30 s, and 72 °C for 1 min, followed by 72 °C for 15 min. The *AmCaM* open reading frame (ORF)

was subcloned into the pTWIN1 vector at the *Not*I and *Pst*I restriction enzyme sites (pTWIN1-AmCaM) and introduced into the *E. coli* strain (ER2566) to generate the putative recombinants. The recombinant plasmid pTWIN1-CaM was transformed into *E.coli* and three clones that grew well in medium containing ampicillin were selected. The three clones harboring the recombinant plasmid were validated by PCR, double digestion and sequencing (Fig. S1).

Expression of *AmCaM* in *E. coli* cells and purification of the recombinant protein

The pTWIN1-CaM and empty pTWIN1 plasmids were inserted into *E. coli* cells (strain ER2566) to generate putative recombinants. For each plasmid, a single colony was used to inoculate Luria–Bertani (LB) medium containing ampicillin (100 mg mL^{-1}). Cultures were incubated at 37 °C for 12 h with shaking (160 rpm). Fresh LB medium (with ampicillin) was inoculated with 0.1% of the bacterial culture and then incubated as before until the optical density at 600 nm reached 0.6. After removing a 1.0-mL aliquot of culture (i.e., control), the remaining *E. coli* cells were treated with 1 mM isopropyl β-D-thiogalactopyranoside (IPTG) and incubated at 37 °C for 3 h. The bacterial cells were divided into two samples. One sample was collected by centrifugation, resuspended in Buffer I [20 mM Tris–HCl (pH 8.5), 500 mM NaCl, and 1 mM EDTA], sonicated to lyse cells, and boiled for 10 min. The lysate was centrifuged at 13,400×*g* for 10 min and the supernatant was collected for a sodium dodecyl sulfate polyacrylamide gel electrophoresis (SDS-PAGE) analysis. The other part of bacteria were collected by centrifugation and resuspended in Buffer II [20 mM Tris–HCl (pH 7.0), 500 mM NaCl, 1 mM EDTA] and stored overnight. Cells were lysed by ultrasonic fragmentation and boiled for 10 min. The heat-unstable proteins were removed by centrifugation (Shi et al. 2016). Clarified cell extract samples were collected for SDS-PAGE analysis. The protein concentration was determined following the method of Bradford (1976).

Assessment of freezing or heat tolerance of *E. coli* cells expressing *AmCaM*

Escherichia coli cells cultured and treated with IPTG as described in the previous section underwent 0–6 freeze–thaw cycles (15 s each) involving liquid nitrogen. Additionally, samples were exposed to 50 °C for 0, 20, 40, 60, 80, or 100 min. Cells for both treatments were diluted appropriately and used to inoculate agar-solidified LB medium containing ampicillin (in triplicate). Cell viability was estimated by counting the number of colony-forming units after an overnight incubation at 37 °C. The mean of three experiments was calculated with at least two independent transformants (with the standard deviation being < 5% in all cases).

Statistical analysis

The survival ratio assay and gene expression measurement were carried out in triplicate. In order to determine the differences, a multiple comparison test of "Least Significant. Difference (LSD) Test" was used. STATISTICA (ver: 6.0) and SPSS (ver: 13.0) programs were used for statistical analyses. The values shown in figures were mean value ± SD.

Results

Analysis of the *AmCaM* cDNA and predicted amino acid sequence

The full-length *AmCaM* cDNA was 753 bp and the ORF sequence (Fig. 1a) encoded a protein with 149 amino acids (63.09% α-helix, 24.16% random coil, 8.05% β-turn, and 4.70% extended strand, with no β-bridge) (Fig. 1b). The molecular weight and theoretical isoelectric point of AmCaM were 25.92 kDa and 4.12, respectively. Additionally, the hydrophilic (ProtScale) AmCaM protein included a signal peptide cleavage site between amino acid positions 29 and 30, and may be localized to the cytoplasm (Fig. 1c).

Sequence homologies and phylogenetic relationship

The AmCaM amino acid sequence was revealed to be 97% identical to the CaM protein sequences from 50 other plant species (Fig. 2a). Previous studies confirmed that CaM consists of multiple isoforms and is highly conserved in yeast and plants (Benoit et al. 2006). Our sequence alignment indicated that AmCaM differs from the homologous proteins in other plant species at three amino acid positions, namely Glu 8, Ala 11, and Val 37. Of the aligned proteins, AmCaM was the only one to contain Val 37 instead of Met 37. Meanwhile, the Glu and Ala residues at positions 8 and 11 of AmCaM were Asp and Ser, respectively. Considering both Ala and Val are hydrophobic residues, the difference between Ser 11 and Met 37 may play a more prominent role in determining the CaM oligomerization states than Ala and Val.

The phylogenetic tree constructed based on the alignment of 50 CaM sequences comprised five branches, with AmCaM placed in the earliest-diverging lineage, implying that it is relatively ancient and conserved. Interestingly, the phylogenetic tree revealed that AmCaM is most closely related to a homolog from *Oryza sativa* Japonica Group (NP_001055907.1) (Fig. 2b), but is also evolutionarily closely related to a homolog from *Vigna angularis*, which

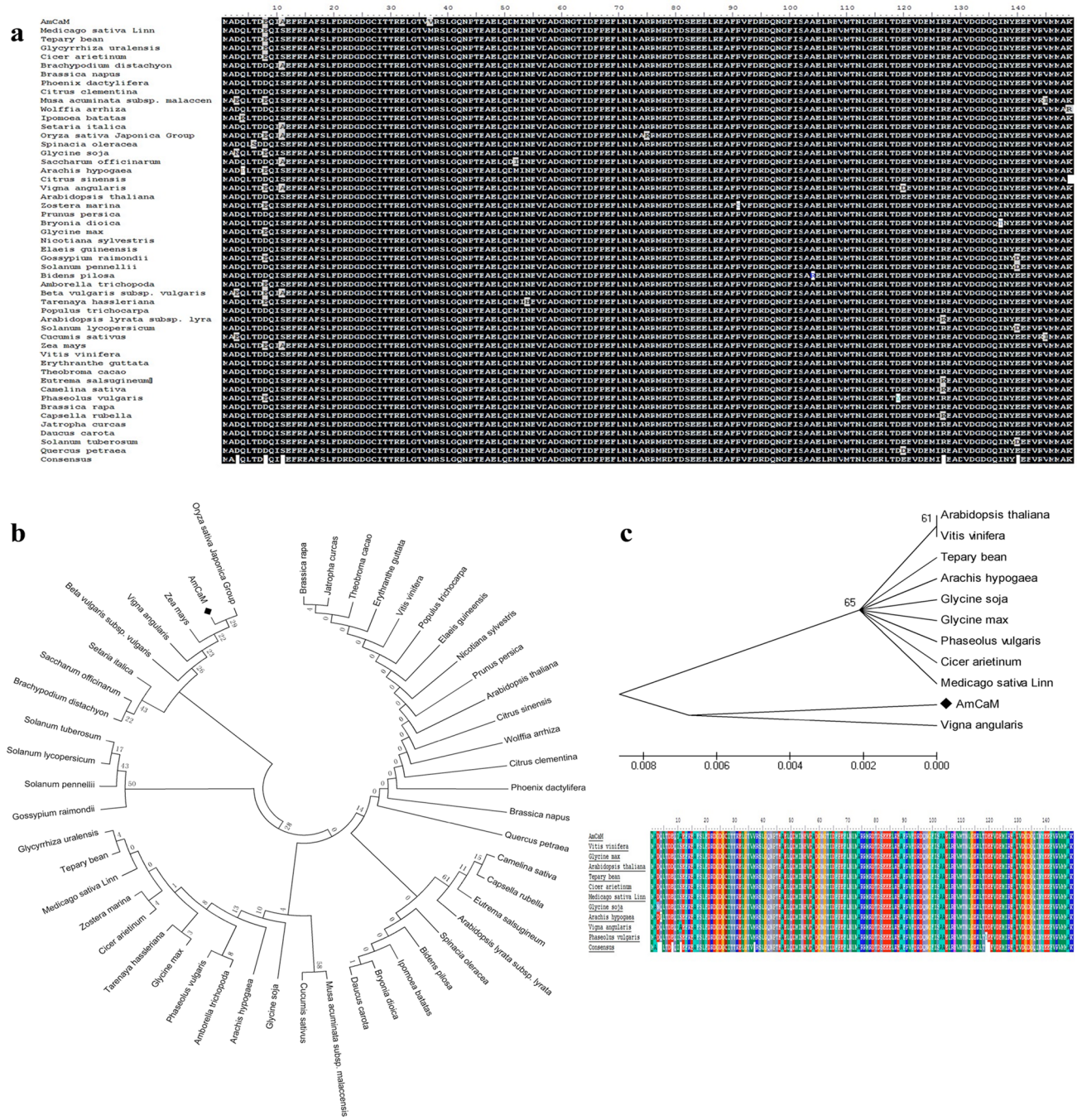

Fig. 2 Comparative analysis of CaM amino acid sequences. **a** Alignment of the deduced AmCaM amino acid sequence with the sequences of homologous CaM proteins from 50 plant species. **b** Maximum likelihood phylogenetic tree indicating the relationships between AmCaM and CaM proteins from other plant species. **c** Neighbor-joining tree representing the relationships between AmCaM and homologous proteins from other leguminous species, *Arabidopsis thaliana*, and grapevine. (Color figure online)

is a leguminous species. We completed a neighbor-joining analysis to further characterize the relationships between AmCaM and the CaMs from other leguminous species (Fig. 2c). Homologs from *A. thaliana* and grapevine (*Vitis vinifera*) were selected as the outgroup. We observed that AmCaM and the homolog from *V. angularis* are closely

related, whereas the homologs from other leguminous plants form a distinct lineage, which includes the outgroup.

AmCaM is responsive to cold and heat stresses

We analyzed the *AmCaM* expression pattern in *A. mongolicus* seedlings subjected to cold and heat stresses using qRT-PCR (Fig. 3). Leaf *AmCaM* expression levels were up-regulated within 1 h of initiating the cold or heat treatment, and peaked at 2 h. Notably, *AmCaM* expression was induced more by cold stress (4 °C) than by heat stress (40 °C) during the first 4 h of treatment. These results suggest that AmCaM may involve in *A. mongolicus* responses to abiotic stresses.

Expression of *AmCaM* in *E. coli* cells

SDS-PAGE analysis showed the presence of the fusion protein in the supernatant of sonicated cell lysates of the transformed cells. The fusion protein Ssp-AmCaM was sensitive to temperature and pH 7.0, and was readily broken into two independent peptides. Hence, to purify the AmCaM protein, Buffer II (pH 7.0) was used for sonication and lysis of the bacterial cells, and purification of the heat-sensitive protein. SDS-PAGE showed that the molecular weight of the expressed protein was 16.81 kDa (Fig. 4c). However, the molecular weight of the expressed product from the soluble fusion protein was about 25.92 kDa (Fig. 4a, b). The difference in molecular weight between the fusion and target proteins was mainly attributable to the pTWIN1 vector expressed in the fusion protein. Consistent with their construction (Fig. S1), the Ssp-Mxe inteins fusion protein and Ssp-*AmCaM* fusion protein were detected in the Ep cells and SA cells, respectively (indicated by white arrows in Fig. 4a, b). Accumulation of the expressed fusion protein in SA1 cells after the induction of IPTG peaked after culture for 3 h at 37 °C (Fig. 4). This finding showed that the Ssp-*AmCaM* fusion protein is a type of soluble protein with no inclusion formation that accumulated at 37 °C.

Expression of *AmCaM* in *E. coli* cells

Our SDS-PAGE results confirmed the presence of the recombinant fusion protein in the supernatants of cell lysates prepared from transformed cells. The Ssp-AmCaM fusion protein was sensitive to heat and buffers of pH 7.0 and pH 8.0, and was readily degraded into two peptides. Hence, to purify AmCaM, bacterial cells were suspended in Buffer II (pH 7.0) prior to being sonicated. Additionally, according to the SDS-PAGE, the purified AmCaM was 16.81 kDa (Fig. 4c), while the soluble fusion protein was about 25.92 kDa (Fig. 4a, b). The difference in molecular weight between the fusion and target proteins was mainly attributable to the pTWIN1 vector expressed in the fusion protein. Consistent with their construction (Fig. S1), the Ssp-Mxe inteins fusion protein and Ssp-*AmCaM* fusion protein were detected in the Ep cells and SA cells, respectively (indicated by white arrows in Fig. 4a, b). Accumulation of the expressed fusion protein in SA1 cells after the induction of IPTG peaked after culture for 3 h at 37 °C (Fig. 4). This finding showed that the Ssp-AmCaM fusion protein is a type of soluble protein with no inclusion formation that accumulated at 37 °C.

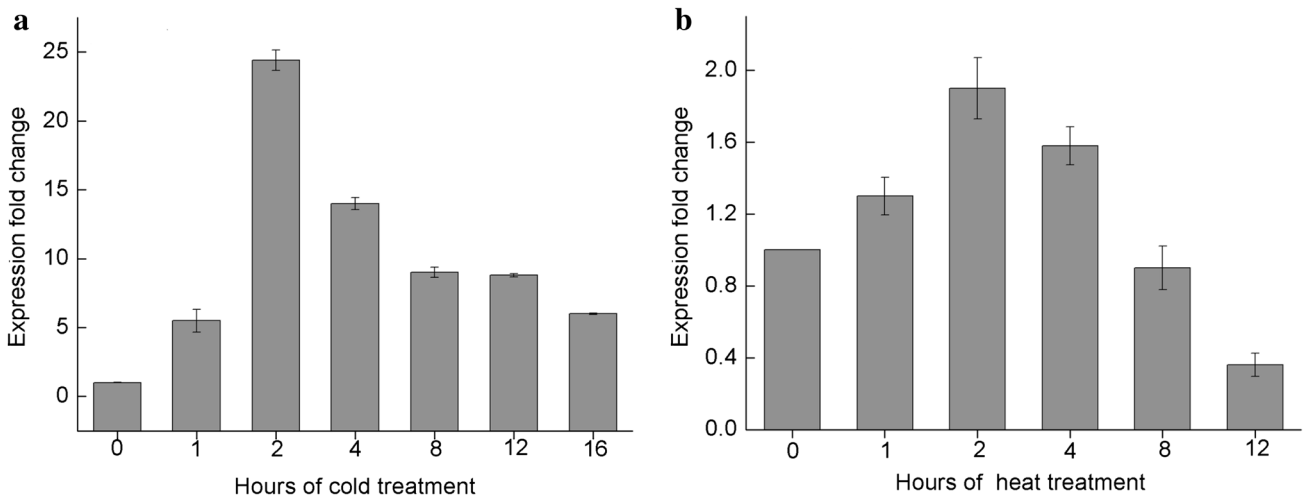

Fig. 3 Analysis of *AmCaM* transcript levels in response to **a** cold and **b** heat stresses at various time points

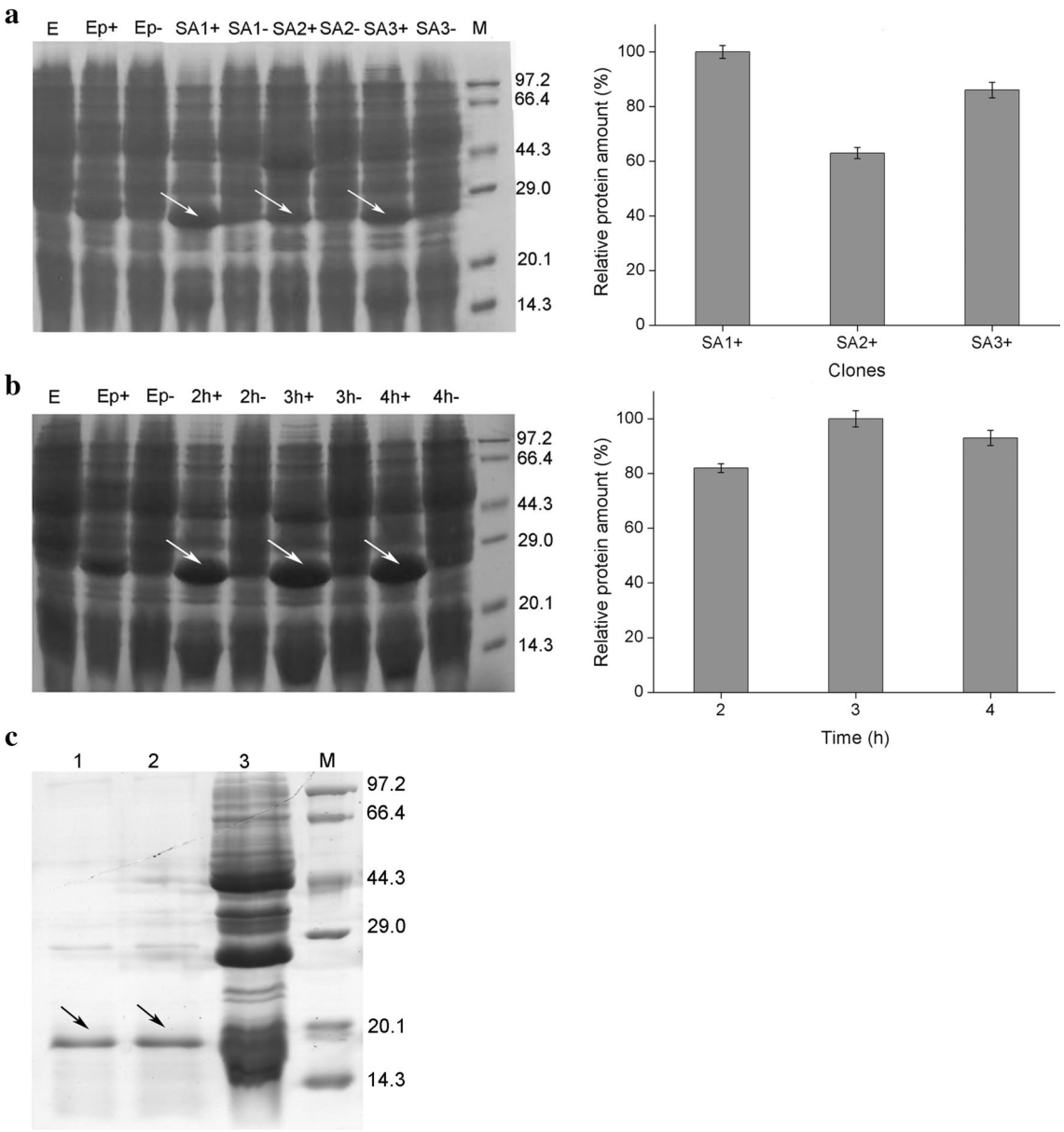

Fig. 4 Results of the SDS-PAGE analysis of *AmCaM* expression in various *E. coli* (ER2566) clones at different time points after adding IPTG. White arrows indicate the band for the AmCaM fusion protein. M, Molecular weight marker; E, non-transformed *E. coli* ER2566 cells; Ep, ER2566 cells transformed with pTWIN1; SA1, SA2, and SA3: different clones of ER2566 cells transformed with pTWIN-AmCaM; +: IPTG added; −: no IPTG. **a** Left: SDS-PAGE analysis of *AmCaM* overexpression in *E. coli* ER2566 cells. Right: relative fusion protein abundance; SA1+, SA2+, and SA3+: different recombinant clones induced by IPTG. **b** Left: SDS-PAGE analysis of *AmCaM* overexpression in *E. coli* ER2566 cells at different time points after adding IPTG. 2, 3, and 4 h: pTWIN-AmCaM recombinant clone 1 at different time points after adding IPTG. Right: relative fusion protein abundance; 2, 3, and 4: AmCaM abundance in transformed clone 1 cells induced by IPTG for 2, 3, or 4 h, respectively. **c** Purification of AmCaM. Lanes 1 and 2: purification of AmCaM, which is indicated with black arrows. Lane 3: SA2+, recombinant clone induced by IPTG

Overexpression of *AmCaM* increases the tolerance of *E. coli* to freezing and heat stresses

To further clarify the function of CaM in a woody plant species in response to abiotic stress and to determine whether AmCaM enhances cellular responses to freeze–thaw cycles or heat stress, cell survival was evaluated for IPTG-induced *E. coli* cells transformed with pTWIN1 (EP+) or pTWIN1-AmCaM (SA+) (Fig. 5). The survival rates of the SA+ and EP+ cells decreased as the number of freeze–thaw cycles increased (Fig. 5a). However, the survival rate of SA+ cells was higher than that of EP+ cells after 1–4 freeze–thaw

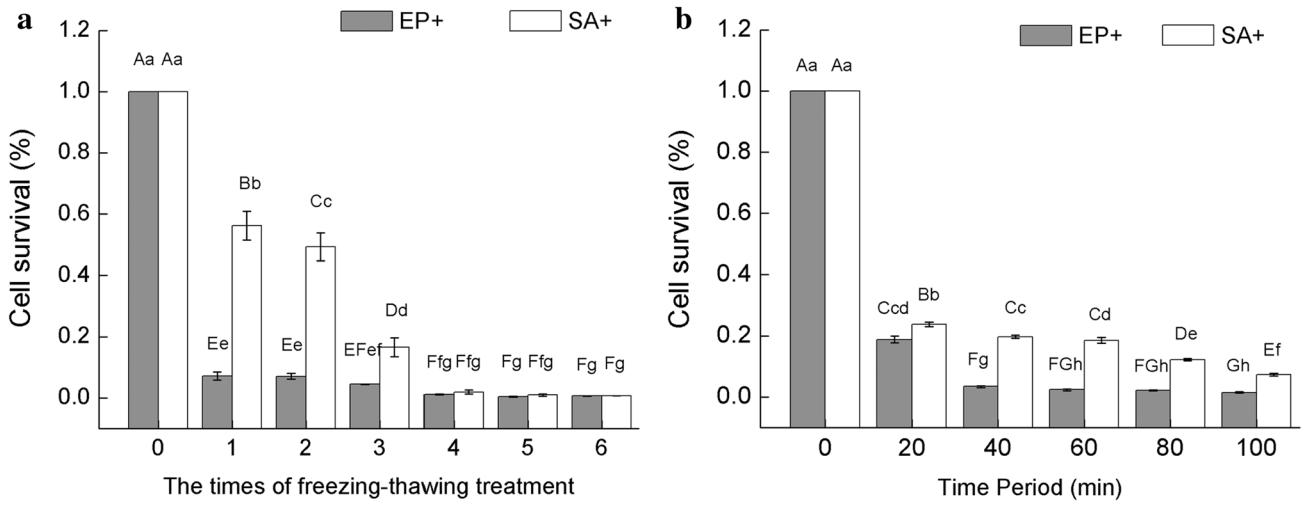

Fig. 5 Tolerance of *E. coli* cells expressing *AmCaM* to **a** freeze–thaw and **b** heat treatments. EP: *E. coli* ER2566 cells transformed with pTWIN1 (control); SA: *E. coli* ER2566 cells transformed with pTWIN1-AmCaM; +: IPTG added. Data are presented as the mean ± standard deviation ($n = 3$). Lowercase and uppercase letters correspond to $P \leq 0.05$ and $P \leq 0.01$, respectively

cycles. A similar phenomenon was observed for the heat treatment (Fig. 5b). These results suggest that *AmCaM* was expressed in the transformed *E. coli* cells, leading to enhanced tolerance to freezing and heat treatments. Furthermore, the survival rate of the SA+ cells was higher after one and two freeze–thaw cycles than after any of the heat treatments (Fig. 5).

Discussion

Calmodulin plays an important role in eukaryotic cell functions and contains typical EF-hand and Ca^{2+}-binding sites (Zeng et al. 2015). We cloned a CaM gene from *A. mongolicus* (Fig. 1), an extremely drought- and frost-resistant plant species. The isolated gene, *AmCaM*, showed high similarity to a homolog from *Oryza sativa* Japonica Group (NP_001055907.1) (Fig. 2b) and was indicated to be a highly conserved gene. The *AmCaM* gene contains four EF hand motifs and specific Ca^{2+}-binding sites, namely aspartic acid (Asp), asparagine (Asn) and glutamic acid (Glu). These three amino acid residues are hydrophobic, which may form a hydrophilic structure (thus increasing protein fluidity). Sequence alignment showed that sites 11 and 37 were converted from the hydrophobic amino acids Ala and Val to the hydrophilic Ser and Met, respectively. This conversion may increase the hydrophilicity of AmCaM and the Met residue adds a sulfur atom to AmCaM. Currently, there is little evidence that CaMs contain a sulfur atom, so the significance of this mutation is unknown.

Calmodulin play essential role in cellular responses to environmental changes (AL-Quraan et al. 2010). We observed an increase in *AmCaM* transcription in response to heat and cold stresses (Fig. 3). In previous studies, cloned *A. mongolicus* cold- and drought-responsive genes also exhibited up-regulated expression in host plants exposed to abiotic stress conditions (Rao et al. 2014; Shi et al. 2016). The root and shoot expression levels of nine *A. thaliana CaM* genes increased by 2–8-fold after a 2-h treatment at 42 °C, with the exception of *CAM1* in the shoots and *CAM5* in the roots and shoots (AL-Quraan et al. 2010). Additionally, the expression of the sweet potato *CaM* gene, *SPCAM*, is significantly up-regulated by NaCl in a dose-dependent manner (Chen et al. 2012). Meanwhile, the expression of the rice CaM gene, *OsCam1-1*, is reportedly up-regulated after 1–3-h treatments with osmotic and salt stresses (Chin et al. 2012). Thus, *CaM* genes form a ubiquitous gene family that contribute to the adaptation of plants to diverse stresses. Accordingly, we proposed that *AmCaM* is a positive regulator of different abiotic stress signaling pathways, which allows *A. mongolicus* to defence the persistent arid environment.

We expressed *AmCaM* in *E. coli* cells to functionally characterize this gene (Fig. 4). The growth rates and stress tolerances were higher for the *E. coli* cells expressing *AmCaM* than for the bacterial and vector controls, implying that AmCaM is involved in enhancing stress tolerance (Fig. 5). Meanwhile, an earlier study confirmed that the expression of the *A. mongolicus LEA* gene differentially affects the tolerance of *E. coli* cells to cold and heat stresses (Liu et al. 2010). Similarly, recombinant *E. coli* cells producing the OsLEA5 fusion protein reportedly exhibit enhanced tolerance to diverse abiotic stresses (e.g., high salinity, osmotic stress, freezing, heat, and ultraviolet radiation) (He et al. 2012). Furthermore, *E. coli* cells transformed with the

salt stress-inducible *SbUSP* gene from *Salicornia brachiata* were observed to have higher survival and growth rates than non-transformed controls following exposures to salt and osmotic stresses (Udawat et al. 2014). These studies revealed that the expression of specific plant genes in bacterial host cells leads to increased stress tolerance. This may be due to the analogous protective mechanisms existing in eukaryotes and prokaryotes under stress conditions (Yun and Zheng 2005; Garay-Arroyo et al. 2000). Calmodulin and Ca^{2+} have been implicated in plant adaptations to different biotic and abiotic stimuli (Virdi et al. 2015). Previous studies indicated that CaM is involved in heat stress signal transductions in wheat (Liu et al. 2003) and *A. thaliana* (Zhang et al. 2009). Moreover, a recent investigation concluded that the overexpression of a *CaM*-like gene (*ShCML44*) increases the tolerance of transgenic tomato plants to drought, salinity, and cold stresses (Munir et al. 2016). Thus, CaM or CaM-like proteins influence the ability of plants to adapt to adverse environmental conditions by regulating different cellular processes (e.g., signal transductions and modulation of transcription factors). However, "How does *AmCaM* confer *E. coli* freezing and heat tolerance?" is the important issue to be addressed here. There is increasing evidence that Ca^{2+} signals affect diverse cellular processes related to physiology and pathogenesis in bacteria, which have tightly regulated cytosolic Ca^{2+} levels (Norris et al. 1996; Theodorou and Kyriakidis 2012; Shemarova and Nesterov 2014). Proteins capable of binding Ca^{2+} with high affinity, including CaM-like proteins, have also been detected in bacteria (Yonekawa et al. 2005). Calcium-binding proteins are present throughout the lifecycle of prokaryotic cells. They function as Ca^{2+} transporters and are important for maintaining Ca^{2+} homeostasis, modulating the cell cycle, regulating enzyme activity, contributing to signal transductions related to the genome, and affecting adaptive behaviors (Michiels et al. 2002; Shemarova and Nesterov 2014). Therefore, it is plausible to predict that the overexpressed AmCaM represents analogous roles as Ca^{2+} binding proteins in *E. coli* cells and thus conferring heat and freezing stress tolerance.

In conclusion, the present results infer that *AmCaM* might participate in the abiotic stress response, which is of immense importance for biotechnology applications. As a signaling molecule, CaM is known to influence a broad range of downstream events, manipulation of which may result in enhanced tolerance to distinct stresses. Future studies will focus on the molecular and biochemical modes of action of this gene.

Acknowledgements We thank Liwen Bianji, Edanz Editing China (http://www.liwenbianji.cn/ac) for editing the English text of a draft of this manuscript. This work was financially supported by the National Natural Science Foundation of China (31270737), Beijing Municipal Natural Science Foundation (KZ20150020021, 6112016), and the National Science Technology Support Program (2011BAI13B06), 111 Project (B13007) and Program for Changjiang Scholars and Innovative Research Team in University (IRT13047).

References

Abbas N, Maurya JP, Senapati D, Gangappa SN, Chattopadhyay S (2014) *Arabidopsis* CAM7 and HY5 physically interact and directly bind to the HY5 promoter to regulate its expression and thereby promote photomorphogenesis. Plant Cell 26:1036–1052

Ali F, Bano A, Fazal A (2017) Recent methods of drought stress tolerance in plants. Plant Growth Regul 82:363–375

AL-Quraan NA, Locy RD, Singh NK (2010) Expression of calmodulin genes in wild type and calmodulin mutants of Arabidopsis thaliana under heat stress. Plant Physiol Biochem 48:697–702

Bender KW, Snedden WA (2013) Calmodulin-related proteins step out from the shadow of their namesake. Plant Physiol 163:486–495

Benoit R, Didier A, Jean PG (2006) Plant calmodulins and calmodulin-related proteins. Plant Signaling Behav 1(3):96–104

Berridge MJ, Bootman MD, Roderick HL (2003) Calcium signalling: dynamics, homeostasis and remodeling. Nat Rev Mol Cell Biol 4:517–529

Boonburapong B, Buaboocha T (2007) Genome-wide identification and analysis of the rice calmodulin and related potential calcium sensor proteins. BMC Plant Biol 7:4

Bradford MM (1976) A rapid and sensitive method for the quantitation of microgram quantities of protein using the principle of protein dye binding. Anal Biochem 6:3177–3188

Chen HJ, Lin ZW, Huang GJ, Lin YH (2012) Sweet potato calmodulin *SPCAM* is involved in salt stress-mediated leaf senescence, H_2O_2 elevation and senescence associated gene expression. J Plant Physiol 169:1892–1902

Chinpongpanich A, Limruengroj K, Phean-O-Pas S, Limpaseni T, Buaboocha T (2012) Expression analysis of calmodulin and calmodulin-like genes from rice, *Oryza sativa L.* BMC Res Notes 5:625

Das A, Ray R, Mandal N, Chakrabarti K (2016) An analysis of transcripts and enzyme profiles in drought stressed jute (*Corchorus capsularis*) and rice (*Oryza sativa*) seedlings treated with $CaCl_2$, hydroxyapatite nano-particle and β-amino butyric acid. Plant Growth Regul 79:401–412

Dubrovina AS, Kiselev KV, Khristenko VS, Aleynova OA (2017) The calcium-dependent protein kinase gene VaCPK29 is involved in grapevine responses to heat and osmotic stresses. Plant Growth Regul 82:79–89

Fasano JM, Massa GD, Gilroy S (2002) Ionic signaling in plant responses to gravity and touch. J Plant Growth Regul 21:71–88

Garay-Arroyo A, Colmenero-Flores JM, Garciarrubio A, Covarrubias AA (2000) Highly hydrophilic proteins in prokaryotes and eukaryotes are common during conditions of water deficit. J Biol Chem 275: 5668–5674

Gilroy S, Bialasek M, Suzuki N, Gorecka M, Devireddy AR, Karpinski S (2016) ROS, calcium, and electric signals: key mediators of rapid systemic signaling in plants. Plant Physiol 171:1–27

Harmon AC, Gribskov M, Harper JF (2002) CDPKs -a kinase for every Ca^{2+} signal? Trends Plant Sci 5:154–159

He S, Tan LL, Hu ZL, Chen GP, Wang GX, Hu TZ (2012) Molecular characterization and functional analysis by heterologous expression in *E. coli* under diverse abiotic stresses for OsLEA5, the atypical hydrophobic LEA protein from *Oryza sativa* L. Mol Genet Genomics 287:39–54

Kang JJ, Zhao WZ, Zheng Y, Zhang DM, Zhou H, Sun PC (2017) Calcium chloride improves photosynthesis and water status in the C_4 succulent xerophyte *Haloxylon ammodendron* under water deficit. Plant Growth Regul 82:467–478

Liu HT, Li B, Shang ZL, Li XZ, Mu RL, Sun DY, Zhou RG (2003) Calmodulin is involved in heat shock signal transduction in wheat. Plant Physiol 132(3):1186–1195

Liu RL, Liu MQ, Liu J, Chen YZ, Lu CF (2010) Heterologous expression of a *Ammopiptanthus mongolicus* late embryogenesis abundant protein gene (*AmLEA*) enhances *Escherichia coli* viability under cold and heat stress. Plant Growth Regul 60:163–168

Liu MQ, Shi J, Lu CF (2013) Identification of stress-responsive genes in *Ammopiptanthus mongolicus* using ESTs generated from cold- and drought-stressed seedlings. BMC Plant Biol 13:88

Luan S, Kudla J, Rodriguez CM, Yalovsky S, Gruissem W (2002) Calmodulins and calcineurin B-like proteins: calcium sensors for specific signal response coupling in plants. Plant Cell 14:389–400

Michiels J, Xi C, Verhaert J, Vanderleyden J (2002) The functions of Ca^{2+} in bacteria: a role for EF-hand proteins? Trends Microbiol 10:87–89

Munir S, Liu H, Xing Y, Hussain S, Ouyang B, Zhang YY, Li HX, Ye ZB (2016) Overexpression of calmodulin-like (ShCML44) stress-responsive gene from *Solanum habrochaites* enhances tolerance to multiple abiotic stresses. Sci Rep 6:31772

Norris V, Grant S, Freestone P, Canvin J, Sheikh FN, Toth I, Trinei M, Modha K, Norman RI (1996) Calcium signalling in bacteria. J Bacteriol 178(13):3677

Perruc E, Charpenteau M, Ramirez BC, Jauneau A, Galaud JP, Ranjeva R, Ranty B (2004) A novel calmodulin-binding protein functions as a negative regulator of osmotic stress tolerance in *Arabidopsis thaliana* seedlings. Plant J 38:410–420

Rao SS, El-Habbak MH, Havens WM, Singh A, Zheng D, Vaughn L, Haudenshield JS, Hartman GL, Korban SS, Ghabrial SA (2014) Overexpression of *GmCaM4* in soybean enhances resistance to pathogens and tolerance to salt stress. Mol Plant Pathol 15:145–160

Reddy AS, Ben-Hur A, Day IS (2011) Experimental and computational approaches for the study of calmodulin interactions. Phytochemistry 72:1007–1019

Shemarova IV, Nesterov VP (2014) Ca^{2+} signaling in prokaryotes. Microbiology 83(5):431–437

Shi J, Liu MQ, Chen YZ, Wang JY, Lu CF (2016) Heterologous expression of the dehydrin-like protein gene *AmCIP* from *Ammopiptanthus mongolicus* enhances viability of *Escherichia coli* and tobacco under cold stress. Plant Growth Regul 79:71–80

Snedden WA, Fromm H (2001) Calmodulin as a versatile calcium signal transducer in plants. New Physiol 151:35–66

Sun FB, Wei JC, Liu Y, Zhang Y, Ma LL, Fu YW, Liu XM (2011) Isolation, transcription and expression of calmodulin gene CaM in *Betula platyphylla*. Nonwood For Res 29:1–7 **(Chinese)**

Tamura K, Peterson D, Peterson N, Stecher G, Nei M, Kumar S (2011) MEGA5: molecular evolutionary genetics analysis using maximum likelihood, evolutionary distance, and maximum parsimony methods. Mol Biol Evol 28:2731–2739

Theodorou MC, Kyriakidis DA (2012) Calcium channels blockers inhibit the signal transduction through the AtoSC system in *Escherichia coli*. Eur J Pharm Sci 47:84–96

Tian X, He M, Wang Z, Zhang J, Song Y, He Z, Dong Y (2015) Application of nitric oxide and calcium nitrate enhances tolerance of wheat seedlings to salt stress. Plant Growth Regul 77:343–356

Udawat P, Mishra A, Jha B (2014) Heterologous expression of an uncharacterized universal stress protein gene (*SbUSP*) from the extreme halophyte, *Salicornia brachiata*, which confers salt and osmotic tolerance to *E. coli*. Gene 536:163–170

Virdi AS, Singh S, Singh P (2015) Abiotic stress responses in plants: roles of calmodulin-regulated proteins. Front Plant Sci 6:809

Wang WJ, Chen YZ, Liu MQ, Lu CF (2008) Effects of cold hardening on compatible solutes and antioxidant enzyme activities related to freezing tolerance in *Ammopiptanthus mongolicus* seedlings. For Stud China 10:101–106

Xu L, Liu ZY, Lu Q, Liang J, Zhang XY (2014) Cloning and expression characteristics of *Pinus massoniana* pmCaM response to *Bursaphelenchus xylophilus* infection. For Res 27:323–328 **(Chinese)**

Yonekawa T, Ohnishi Y, Horinouchi S (2005) A calmodulin-like protein in the bacterial genus *Streptomyces*. FEMS Microbiol Lett 244: 315–321

Yun L, Zheng Y (2005) PM2, a group 3 LEA protein from soybean, and its 22-mer repeating region confer salt tolerance in *Escherichia coli*. Biochem Biophys Res Commun 331:325–332

Zeng HQ, Xu LQ, Singh AJ, Wang HZ, Du LQ, Poo BW (2015) Involvement of calmodulin and calmodulin-like proteins in plant responses to abiotic stresses. Front Plant Sci 6:600

Zhang W, Zhou RG, Gao YJ, Zheng SZ, Xu P, Zhang SQ, Sun DY (2009) Molecular and genetic evidence for the key role of AtCaM3 in heat-shock signal transduction in Arabidopsis. Plant Physiol 149:1773–1784

Zhu X, Dunand C, Snedden W, Galaud JP (2015) CaM and CML emergence in the green lineage. Trends Plant Sci 20:483–489